

# Dissipation of Magnetic Fields in the Galactic Halo

*Dedicated to Professor Karl Schindler on the occasion of his 65th birthday*

F. Zimmer<sup>1</sup>, H. Lesch<sup>2</sup>, G.T. Birk<sup>2</sup>

<sup>1</sup> Radioastronomisches Institut der Universität Bonn, Auf dem Hügel 71, D-53121 Bonn, Germany

<sup>2</sup> Institut für Astronomie und Astrophysik der Universität München, Scheinerstraße 1, D-81679 München, Germany

Received June 27, accepted October 4, 1996

**Abstract.** This paper shows that magnetic reconnection could be an important heating process in cosmic gases. In any volume where magnetized plasmas collide, the dissipation of magnetic energy via reconnection seems to be unavoidable. Since most cosmic plasmas are highly conductive, the magnetic field lines are transported with the gas and no dissipation occurs for the most part of the volume. This ideal frozen-in property of the magnetic field is broken in small volumes if field gradients with different field polarity appear, in which localized dissipative effects, e.g. anomalous resistivity, become important. On the base of X-ray measurements exhibiting a clear connection of infalling high-velocity clouds (HVC) with ROSAT "hotspots" we perform resistive magnetohydrodynamic simulations to investigate the capabilities of magnetic dissipation as a major heating process in the interaction zone of the cloud with the halo. The main result is that in the physical environment of a galactic halo heating by externally driven magnetic reconnection cannot be suppressed by thermal conduction and/or radiative cooling. Thus, the gas reaches the maximum temperature given by the magnetic field pressure in the interaction zone of the HVC with the galactic halo.

**Key words:** Magnetic Reconnection – Magnetohydrodynamics – Microinstability – Numerical Methods

## 1. Introduction

Radio observations clearly reveal that the halo of the Milky Way is a magnetized plasma (Haslam et al. 1982). The radio emission is due to nonthermal synchrotron radiation of relativistic electrons gyrating around a magnetic field with an average field strength of several  $\mu\text{G}$  (Beuermann, Kanbach and Berkhuijsen 1985). The relativistic

particles move through a fully or partially ionized plasma, which consists of several gas components, starting from HI with temperatures of some 100 K and extending up to X-ray emitting gas with temperatures of about a million K (e.g. Lesch et al. 1996 for a recent conference about the galactic halo). The halo gas is agitated by the activity in the disk (supernova remnants, stellar winds, bubbles and superbubbles, etc.), which led to the picture of Galactic Fountain (e.g. Kahn 1981). This fountain is formed by hot gas rising from the galactic disk. At some height the gas starts to cool and may partially fall back onto the disk in form of high-velocity clouds (Kahn 1991). Thus, the halo gas may also be agitated by the recurrent high-velocity clouds. Such HVCs have been observed long before the scenario of galactic fountains was developed (Muller et al. 1963) and it was anticipated that they interact with the halo gas or the disk itself (Oort 1970). One should expect that the interaction should reveal itself by some enhanced radiation originating from heated gas.

Hirth et al. (1985) first announced the detection of a HVC associated with soft X-ray emission close to the Draco cloud, which itself may be interpreted as the result of a HVC-disk interaction (Mebold et al. 1989). Since their data covered only the  $\frac{1}{4}$  keV energy range which is heavily disturbed by absorption of neutral matter distributed along the line of sight, their detection was not completely convincing.

Kerp et al. (1994) found clear evidence for the association of the HVC with  $\frac{3}{4}$  keV X-ray emission, which cannot be significantly attenuated by absorption. They also detected a detailed anticorrelation of HVC and X-ray emission. In a recent paper Kerp et al. (1996) were able to show that large parts of the HVC complex C are associated with soft X-ray radiation. With the new Leiden-Dwingeloo HI-survey (Hartmann and Burton 1995) they could prove that the HVC velocity regime is connected with low-velocity atomic hydrogen of the galactic disk by velocity bridges. In other words the impacting HVC gas is dragged by the halo. This interpretation is corroborated

---

*Send offprint requests to:* F. Zimmer

by positional correlation of the HI velocity bridges with the soft X-ray enhancement. Thus, the edges of the HVC are sources of strong X-ray emission, revealing a gas temperature of a few million degrees.

The striking conclusion that an impacting HVC is responsible for the local X-ray emission raises the question about the physical mechanism which releases the observed luminosity of about  $10^{32}$  erg s $^{-1}$ . An inelastic collision of the HVC with the galactic disk converts kinetic energy into thermal energy (Hirth et al. 1985). But this ram pressure process is unlikely the source of the X-rays even of the  $\frac{3}{4}$  keV emission, because most of the HVC models predict velocities that are approximately equal in all three spatial directions and of about 100 km s $^{-1}$  (Mebold et al. 1991). Therefore, the complete kinetic energy of the cloud has to be transformed into heat in order to reach the observed few million K.

In Fig. 1 we sketch the scenario we have in mind. A HVC hits the Reynolds layer (Reynolds 1991), which consists of an ionized, magnetized hydrogen plasma. We assume that the magnetic field in the halo is preferentially directed parallel to the disk, which usually is the case for spiral galaxies (Dumke et al. 1995).

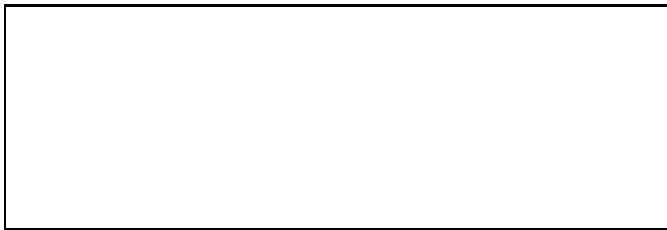


**Fig. 1.** A HVC collides with the Reynolds layer, an ionized hydrogen layer of the galactic halo which includes magnetic fields

It is the aim of this contribution to investigate the probable braking mechanisms for the HVC. Even though the impact velocities are of the order of the sound speed for a gas of one million degree Kelvin, shock heating does not provide a sufficiently efficient mechanism for X-ray temperatures (Zimmer et al. 1996). In Section 2 we introduce magnetic reconnection as a major heating process in the interstellar medium. The interaction of HVCs with the galactic disk can be considered as a prime example for this process. Section 3 contains the details of the resistive magnetohydrodynamic simulations of the cloud impact onto the galactic disk. Several cooling processes competing with the magnetic heating are considered in Section 4. Finally, we sum up our findings in Section 5.

## 2. Magnetic dissipation

It is well known that magnetic fields contribute significantly to the interstellar pressure and energy reservoir.

Most of the interstellar plasma is highly conductive, i.e. we can write Ohm's law  $\mathbf{E} + (\frac{1}{c}\mathbf{v} \times \mathbf{B}) = 0$  (if we neglect the Hall term, electron pressure term and inertia terms for simplicity). In this case the magnetic field is "frozen" in the plasma and transported by plasma flows. This property of the magnetic field changes drastically, e.g. if field lines with different directions approach each other and localized dissipative regions form. The chain of processes which is triggered then is called **magnetic reconnection** (e.g. Priest 1985; Biskamp 1994 and references therein).

Magnetic reconnection is a fundamental intrinsic property of agitated magnetized plasmas with a non-zero electric field component along the magnetic field (e.g. Schindler et al. 1991). Whenever, magnetic fields with different field directions encounter, the magnetic energy can partly be dissipated, either by accelerating particles or by plasma heating. The approaching field lines correspond to parallel currents which attract each other. Outside the forming current sheet the motion of the plasma is "frozen-in", i.e. the magnetic field lines follow the plasma motion as if they were frozen into it, which is provided by the high electrical conductivity. The oppositely directed field lines following the plasma motion approach, the field gradient steepens and the current density  $\frac{c}{4\pi}\nabla \times \mathbf{B}$  increases until strong dissipation sets in. Different from mere diffusion that occurs on a time scale given by  $\tau_D = L_o^2/\eta$  reconnection is a rather fast localized dissipative process involving global changes in magnetic field topology. The problem of reconnection is to know how the dissipation of the currents with the density  $j = en_e v_d$  is provided ( $n_e$  is the electron number density per cm $^3$  and  $v_d$  denotes the drift velocity of the electrons relative to the protons.)

Since magnetic reconnection seems to be unavoidable in plasmas with randomly mixed magnetic fields we propose that the encounter of a high velocity plasma with the "magnetic atmosphere" of the Milky Way transfers the kinetic energy of the clouds into heat via compressed, strained and teared magnetic field structures, which heavily dissipate the stored magnetic energy in current sheets via magnetic reconnection.

Since magnetic reconnection corresponds to the dissipation of electric currents the dissipation (or heating) rate  $Q$  (in erg cm $^{-3}$  s $^{-1}$ ) is

$$Q = \frac{j^2}{\sigma}. \quad (1)$$

Dissipation is equivalent to either increased current density and/or reduced electrical conductivity  $\sigma$

$$\sigma = \frac{\omega_{pe}^2}{4\pi\nu_{coll}}. \quad (2)$$

$\nu_{coll}$  is the collision frequency and  $\omega_{pe} \sim 5.6 \cdot 10^4 \sqrt{n_e}$  is the electron plasma frequency.

We first give a qualitative estimate of kinetic energy conversion into heat via magnetic reconnection and rough

estimates of the heating process. The details of the plasma processes involved have been discussed by Lesch (1991).

The collision of a high velocity gas with the magnetized galactic disk can be described in two ways: as an interaction of two magnetized plasmas, if the HVC contains a magnetic field or otherwise as the interaction of a non-magnetized plasma with a magnetized one, if only the disk is magnetized.

In the first case, the appearance of magnetic reconnection is obvious: the magnetic field lines of the cloud and the field lines of the disk are compressed and randomly mixed in a boundary layer. There is observational evidence that HVCs indeed possess magnetic fields. Kazès et al. (1991) detected a field strength of about  $11\mu\text{G}$  in a HVC via Zeeman measurements.

Pietz et al. (1996) detected HI-velocity-bridges which demonstrate that the clouds velocities continuously decrease with decreasing distance to the disk, i.e. the clouds are slowed down. The size of these bridges indicates that the interaction region between the cloud and the halo has an extension of about  $10'$  or  $4\text{ pc}$  assuming a distance of  $1.5\text{ kpc}$ . Using the Westerbork interferometer Wakker (1991) observed the substructure of HVCs. He found thin dense filaments with an extension of less than  $0.4\text{ pc}$  assuming a distance of  $1.5\text{ kpc}$  again. These filaments reveal turbulent motions inside the boundary layer down to little scales. Kerp & Güsten (1996) confirm this result via Zeeman measurements: They derive a magnetic field strength of  $20 - 30\ \mu\text{G}$ , which changes on small scales inside the cloud.

Thus, we can use about  $10\ \mu\text{G}$  as the value for the unperturbed field strength. If such a magnetized cloud approaches the galactic disk the undistorted field will be compressed until reconnection sets in due to localized dissipative regions, since for most of its path the magnetic field is frozen into the cloud. Such an encounter of two magnetized plasmas could be envisaged as the collision of two magnetized networks. As long as both magnetic field structures collide with some angle reconnection will be driven by the plasma motion of the cloud. A huge number of current sheets will be built up in the whole interaction volume, which are accompanied by dissipation via plasma heating (Lesch and Bender 1990).

In the second case, the magnetic field of the disk will be distorted by the shear flow in the boundary layer between the incoming HVC and the disk. As long as the field is frozen-into the plasma motion the field is mixed and again field lines with different directions will encounter and the kinetic energy of the cloud is transferred into heat via the formation current sheets and Ohmic dissipation.

The physical scenario we have in mind is sketched in Fig. 2. Assuming a distance of the clouds of about  $1.5\text{ kpc}$  the HVC interacts with the Reynolds layer, the ionized hydrogen gas layer of the galactic halo. The clouds themselves are ionized by cosmic rays and the soft-X-ray-background as well. The impact of the cloud into the

Reynolds layer is shown in the left upper figure which represents the most interesting part of the ROSAT-image schematically.

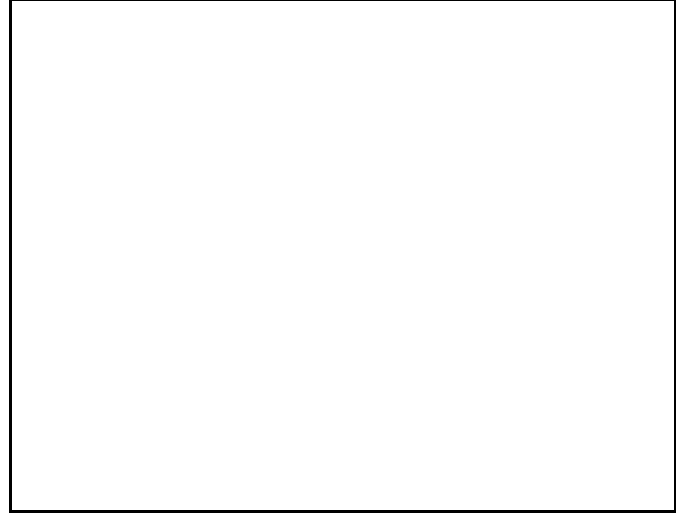


**Fig. 2.** The scenario we have in mind: A HVC interacts with the Reynolds layer and a large number of small scale reconnection sheets is formed.

For both cases the maximum temperature can be estimated by considering the equilibrium between the kinetic energy density and magnetic energy density or thermal energy density, respectively:

$$\frac{1}{2}n_{\text{H}}^{\text{HVC}}m_{\text{p}}v_{\text{HVC}}^2 \simeq \frac{B_0^2}{8\pi} \simeq n_{\text{e}}^{\text{BL}}k_{\text{B}}T_{\text{e}} \quad (3)$$

here  $v_{\text{HVC}}$  is the velocity of the HVC,  $n_{\text{H}}^{\text{HVC}}$  is the neutral density of the HVC and  $n_{\text{e}}^{\text{BL}}$  is the electron density in the boundary layer.  $T_{\text{e}}$  denotes the electron temperature,  $k_{\text{B}}$  is the Boltzmann constant and  $m_{\text{p}}$  is the proton mass.

The resulting temperature is given by

$$T_{\text{e}} \simeq \frac{n_{\text{H}}^{\text{HVC}}}{n_{\text{e}}^{\text{BL}}} \frac{1}{k_{\text{B}}} \frac{1}{2} m_{\text{p}} v_{\text{HVC}}^2 \quad (4)$$

which gives

$$T_{\text{e}} \simeq 6 \cdot 10^6 \text{K} \left[ \frac{v_{\text{HVC}}}{100 \text{ km s}^{-1}} \right]^2 \left[ \frac{n_{\text{H}}^{\text{HVC}}/n_{\text{e}}^{\text{BL}}}{10} \right] \quad (5)$$

We note that the Eq. (5) is an underestimate of the heat transfer since the density contrast  $n_{\text{H}}^{\text{HVC}}/n_{\text{e}}^{\text{BL}}$  is larger than 10 (Wakker 1991).

The attainable temperatures are definitely high enough to explain the edge brightening of the HVC in the X-ray range.

The global energy budget can be estimated as follows: the energy density of the magnetic field  $U = B^2/8\pi$  is dissipated with an efficiency  $\epsilon$  across an area  $A$  of about

(4 pc)<sup>2</sup> (taken from the observations). For the velocity with which energy is converted during the reconnection process ( $v_{diss}$ ) we use a tenth of the velocity of the HVC  $v_{diss} \sim 10 \text{ km s}^{-1}$ . This results in a total luminosity

$$L_{rec} = U \epsilon v_{diss} \sim 10^{33} \frac{erg}{s} \left[ \frac{\epsilon}{0.1} \right] \left[ \frac{B}{10 \mu G} \right]^2 \left[ \frac{v_{diss}}{10 \frac{km}{s}} \right] \left[ \frac{A}{(4 pc)^2} \right] \quad (6)$$

After these qualitative estimates we present in the next section our numerical resistive magnetohydrodynamical simulations.

### 3. Simulation Results

We perform resistive magnetohydrodynamic simulations (for details concerning the code see Otto 1990) to investigate the impact of a magnetized gas cloud onto a magnetized gas. We numerically integrate the set of basic equations:

**Equation of Continuity:**

$$\frac{\partial \rho}{\partial t} = -\nabla \cdot (\rho \mathbf{v})$$

**Momentum Equation:**

$$\frac{\partial}{\partial t} (\rho \mathbf{v}) = -\nabla \cdot (\rho \mathbf{v} \circ \mathbf{v}) - \nabla p + \frac{1}{4\pi} (\nabla \times \mathbf{B}) \times \mathbf{B}$$

**Energy Equation:**

$$\frac{\partial p}{\partial t} = -\mathbf{v} \cdot \nabla p - \gamma p \nabla \cdot \mathbf{v} + (\gamma - 1) \eta \left( \frac{c}{4\pi} \right)^2 (\nabla \times \mathbf{B})^2$$

**Induction Equation:**

$$\frac{\partial \mathbf{B}}{\partial t} = \nabla \times (\mathbf{v} \times \mathbf{B}) - \frac{c^2}{4\pi} \nabla \times (\eta \nabla \times \mathbf{B})$$

Here  $\rho$ ,  $p$ ,  $\mathbf{v}$ ,  $\mathbf{B}$  and  $\eta$  denote the mass density, thermal pressure, plasma velocity, the magnetic field and the resistivity. All quantities are made dimensionless by a normalization to typical parameters. Length scales are normalized to a typical length  $L_o$ ,  $\rho$  is normalized to a mass density  $\rho_o = m_o n_o$  (where we take  $m_o$  to be the ion mass),  $B$  to a typical magnetic field strength  $B_o$ ,  $p$  to  $p_o = \frac{B_o^2}{8\pi}$  and the plasma velocity to the Alfvén velocity  $v_A = \frac{B_o}{\sqrt{4\pi\rho_o}}$ . The time scale is normalized to the Alfvén transit time  $\tau_A = \frac{L_o}{v_A}$ .

Here we present some results of 2 $\frac{1}{2}$ D simulations ( $\partial/\partial z = 0$ ). The resistive MHD-equations above are integrated on a 2D domain shown in Fig. 3.

Initially the magnetic field has the following form:

$$\mathbf{B} = B_i \tanh \left( \zeta \left[ y - \frac{y_{max} + y_{min}}{2} \right] \right) \mathbf{e}_x$$



**Fig. 3.** The MHD-equations are integrated on the 2D area, shown as a dashed plane.

and thus, the current density reads:

$$\mathbf{j} = j_i \operatorname{sech}^2 \left( \zeta \left[ y - \frac{y_{max} + y_{min}}{2} \right] \right) \mathbf{e}_z$$

During the dynamical evolution magnetic flux is transported into the numerical domain, and magnetic field lines of different polarity are compressed. Whenever magnetic fields with different polarity approach, a current sheet is formed. Outside this sheet the motion of the plasma is "frozen in", that means, the magnetic field lines follow the plasma motion as if it were frozen into it. This is due to the high electric conductivity in the plasma outside the current sheet. So, when the plasmas collide, the magnetic field lines follow this motion, the field gradient steepens and the current density  $j \sim \nabla \times \mathbf{B}$  increases significantly. On the other hand  $j$  is proportional to the drift velocity of the electrons  $j \sim nev_D$ , so that  $v_D$  increases with  $j$ .

The growth of the current density, i.e. of the drift velocity is limited by microscopic plasma instabilities (e.g. Sagdeev 1979). If the drift velocity exceeds the thermal velocity of the particles, several wave modes that are excited by pressure gradients or electric currents can grow unstable. The nonlinear saturation phase of these microinstabilities gives rise to electrical resistance mediated by wave-particle interactions. Momentum transfer between the charges species is caused via turbulent electromagnetic fields, i.e. the classical resistivity changes into anomalous resistivity. Since the anomalous collision frequency is considerably larger than the classical Coulomb value, the onset of microturbulence increases the dissipation rate by many orders of magnitude.

We model the effect of anomalous resistivity by:

$$\eta = \eta_o \cdot |\mathbf{j} - \mathbf{j}_c| \cdot \frac{1}{\cosh(\xi x)}$$

if the current density  $|\mathbf{j}|$  exceeds the critical value  $j_c$  ( $\xi$  measures the scale length on which the resistivity vanishes in the  $x$ -direction ( $\frac{1}{\xi} \approx 7 \cdot 10^9 \text{ cm}$ )).

Otherwise the resistivity vanishes.

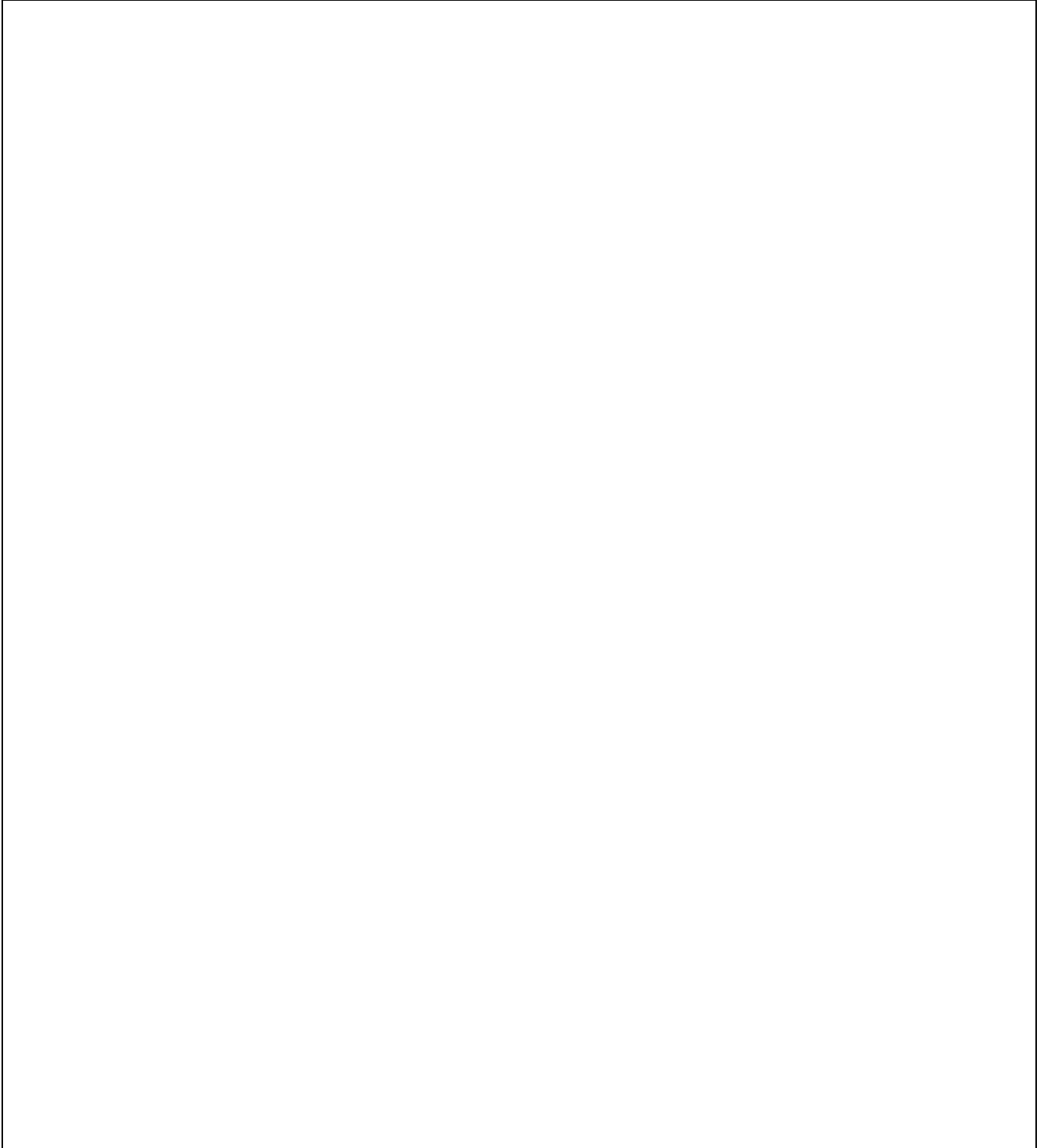


**Fig. 4.** The time development of the number density  $n$  with an initial temperature of  $9 \cdot 10^5$  K and an initial number density of 0.01 particles per  $\text{cm}^3$ . The typical length scale  $L_o$  is about  $1.5 \cdot 10^9$  cm.

The drift velocity is associated with the magnetic field gradient via

$$v_D \simeq \frac{c}{4\pi en_e} \frac{B}{l} \quad (7)$$

Eq. (7) means that the larger the magnetic field gradient is the higher is the drift velocity. So one can expect that in the innermost current sheet plasma waves are excited. We note that in general one has to distinguish between magnetized and unmagnetized instabilities. The former could not appear in the neutral sheet (with  $B = 0$ ). Thus, these instabilities do not directly produce anomalous resistivity in magnetic null regions (details see Lesch 1991).

In what follows we consider unstable lower hybrid drift waves as the mediator for anomalous resistivity in the reconnection region. Such waves are excited by local pressure gradients and grow unstable if the drift velocity associated with these gradients exceeds a critical value. lower hybrid drift instability (LHI). Two properties in favor of this instability are (1) the mode can be excited in relatively broad current sheets since the necessary drift velocity is the thermal velocity of the ions  $l \simeq (\frac{m_i}{m_e})^{1/4} r_{Li}$  (where  $r_{Li}$  is the ion Larmor radius) and (2) the mode is insensitive to the temperature ratio  $\frac{T_e}{T_i}$ . The anomalous collision frequency associated with LHI is approximately equal to the lower-hybrid frequency  $\omega_{LH}$  (e.g. Shapiro et al. 1994, Sotnikov et al. 1978)

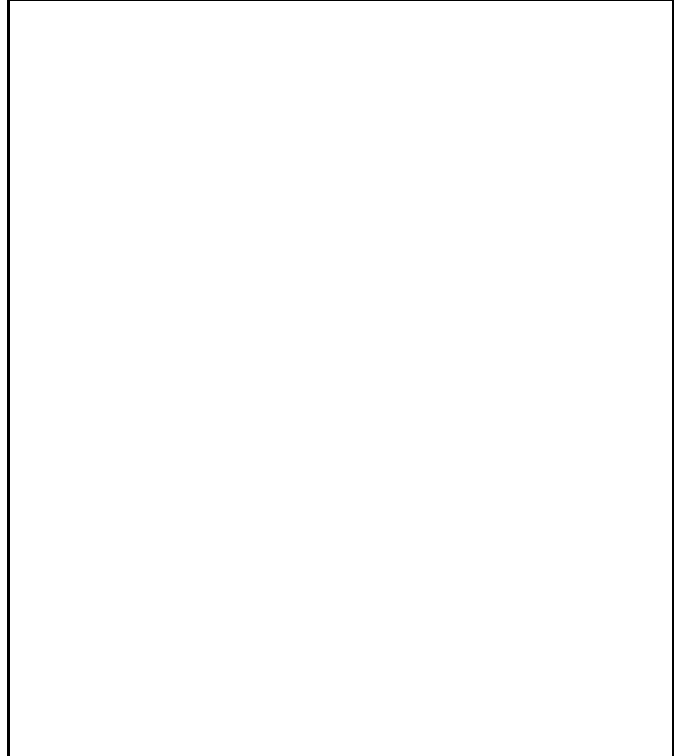
$$\nu_{coll}^{LHI} \simeq \omega_{LH} \simeq 4 \times 10^5 B s^{-1}. \quad (8)$$

Therefore, in the following we assume  $\nu_{coll} \simeq \omega_{LH}$  and  $v_D \simeq v_{thi}$ .

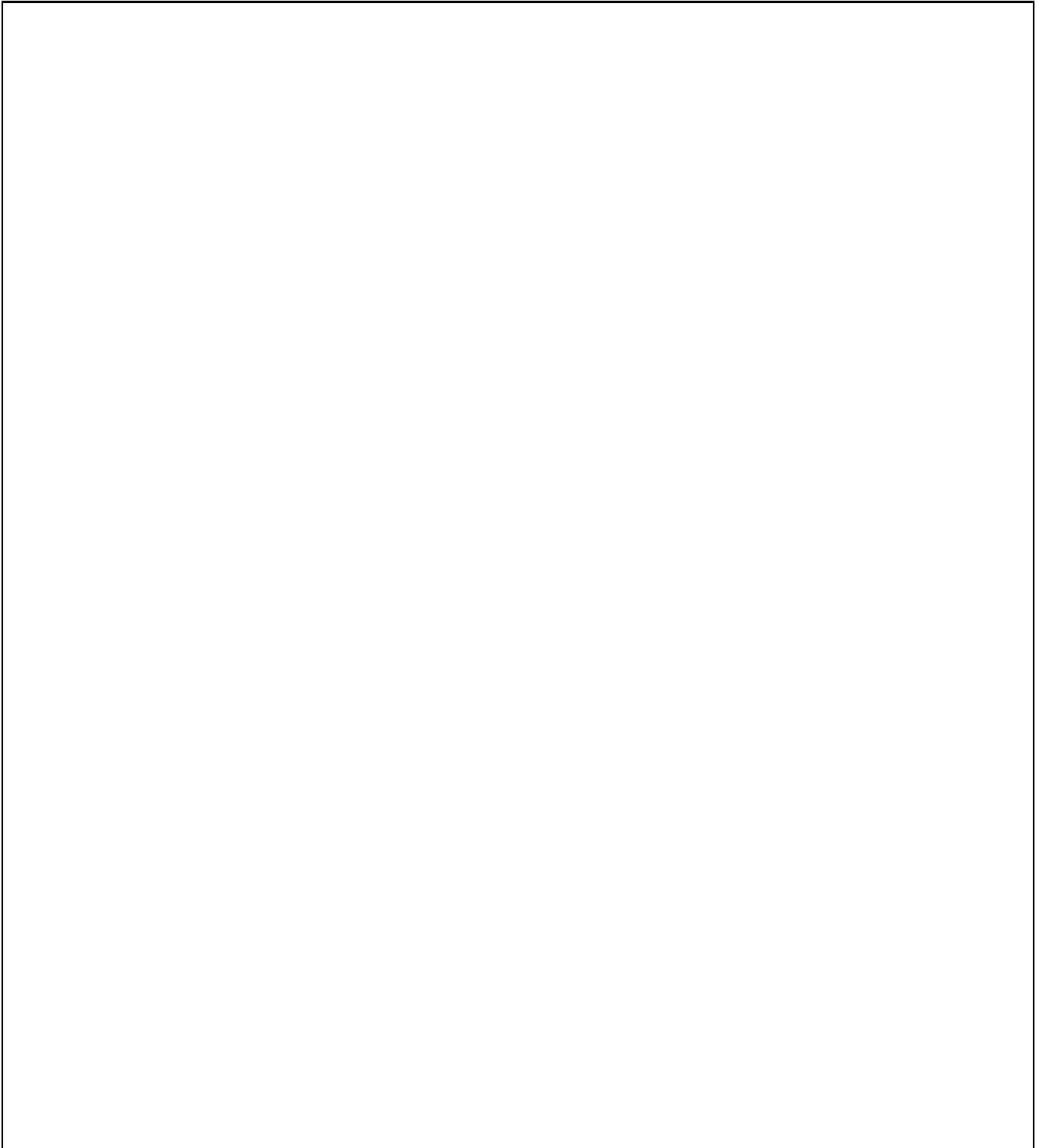
The first example shows a situation, where the initial temperature is about 900 000 K and the initial density is about 0.01 particles per  $\text{cm}^3$ . The initial pressure and initial density are constant. The "global" Alfvén speed is about  $3 \cdot 10^7 \text{ cm s}^{-1}$ ; the magnetic field strength is about  $17 \mu\text{G}$ .

Fig. 4 shows the time development of the number density. The time is given in Alfvén times, one Alfvén time is about 50 sec (for comparison the diffusion time is some  $10^4$  sec). We see that the plasma is compressed by the magnetic field and the density grows very quickly.

Further we see that the density then becomes smaller again inside the reconnection zone. This is because pressure forces and the Lorentz force accelerates the plasma out of the zone. This can be seen in Fig. 5 showing the outflow component of the plasma velocity after 75 Alfvén times, which reaches about 50 - 60 % of the "global" Alfvén speed. The time-development of the magnetic field is illustrated in Fig 6. Magnetic field lines of opposite polarity encounter, the field lines reconnect and the Lorentz forces arising in these configurations accelerate the plasma out of the reconnection zone.



**Fig. 5.** The outflow component of the velocity after 75 Alfvén times



**Fig. 6.** Magnetic field lines of different polarity flow together and they reconnect. “Magnetic islands” form.

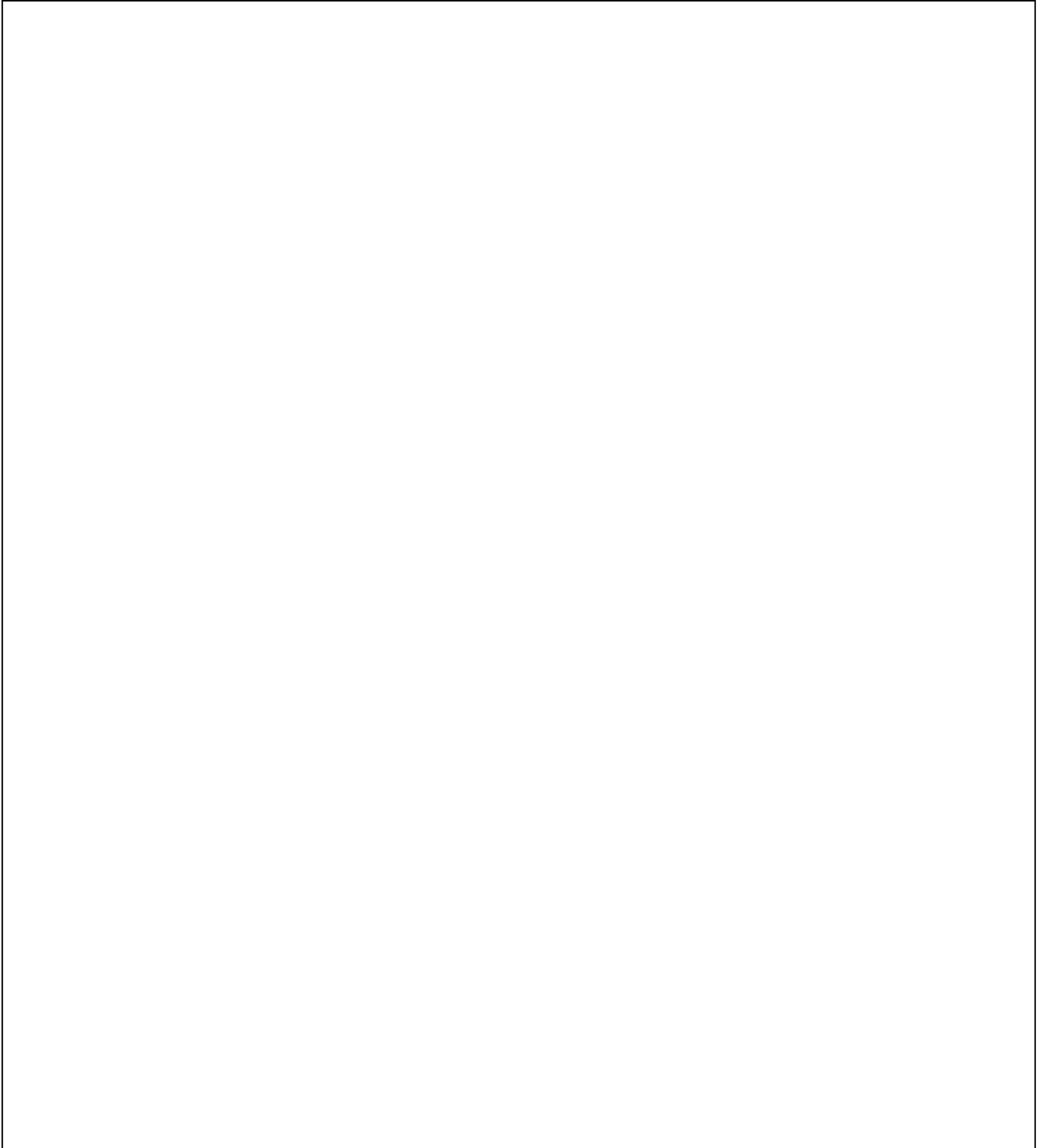


**Fig. 7.** The time development of the corresponding temperature.



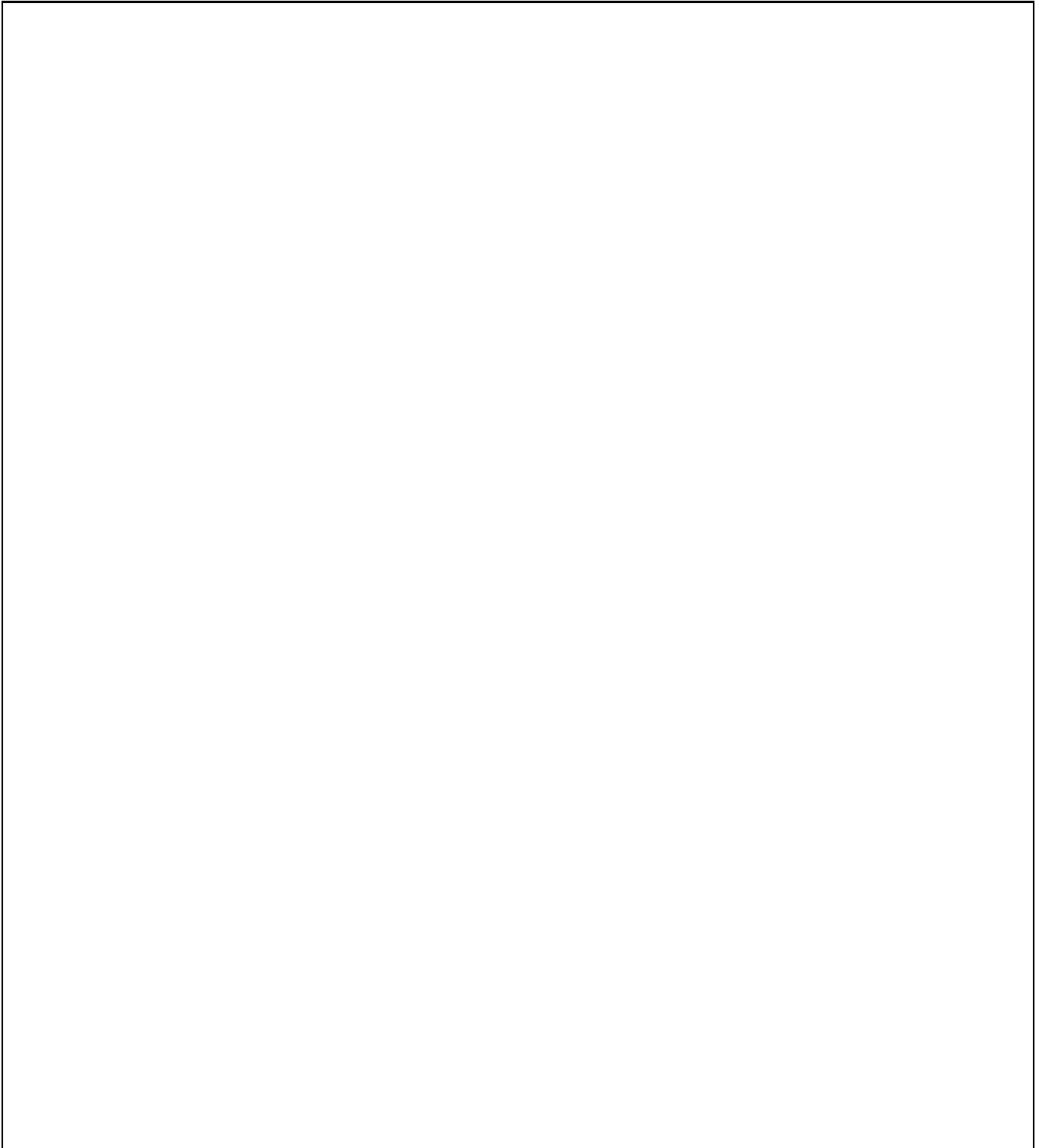


**Fig. 8.** The time development of the temperature in the “low temperature case”.

The temperature reaches the observed temperatures of a few million K degree within a very short time of 1.5 hours (cf. Fig. 7). Two effects can easily be seen:

- The magnetized plasma is compressed, i.e. mass density and temperature are increased.
- The temperature peak is the result of magnetic reconnection.

Both, magnetic compression and magnetic reconnection, lead to the observed temperatures. We note that the plasma flows escaping from the reconnection zones mediate the high temperature information to the surrounding medium. A chain of processes takes place in the plasma around the reconnection zones. First the kinetic energy of the plasma flows is converted into heat and second the plasma flows induce plasma instabilities in the gas. They result in an increase of the collision frequency and a reduction of the electrical conductivity. Additionally, magnetic reconnection leads to a relaxation of the agitated magnetic field.

We started these simulations at nearly one million K degree. However, since the Reynolds layer is much cooler than 900 000 K, we consider also the time development of the temperature for the case, where the initial temperature is about 250 K and the initial density is about 22.5 particles per  $\text{cm}^3$  (Fig. 8). The magnetic field strength is again chosen as  $17 \mu\text{G}$  and the Alfvén time is about 35 sec. Temperatures of more than 2000 K are easily reached within a very short time. Both effects, magnetic compression and magnetic reconnection are clearly visible.

#### 4. Cooling processes

The simulations confirm the qualitative estimates that the plasma can be heated up to a few million K within a very short time. To fill up a large volume with hot gas via magnetic heating the heating process must not be overcome by radiative and thermal conductive losses, the cooling time  $t_{cool}$  and the conductive time  $t_{cond}$  have to be larger than the corresponding heating time  $t_{heat}$ ; if the gas would cool very quickly, magnetic heating could not explain the observations.

The conversion of kinetic energy into luminosity by collision processes cools a hot, partly or totally ionized gas to lower temperatures. The principal cooling mechanism for a very hot plasma with temperature more than  $10^7$  K is thermal bremsstrahlung or free-free emission. Gas at lower temperatures cools mainly by electron impact excitation of electronic levels of the neutral and ionized particles. Finally the fine structure excitation becomes more and more important. Taking all these processes into account, Dalgarno & McCray (1972) derived the interstellar cooling function  $\mathcal{L}$ , shown in the following figure:

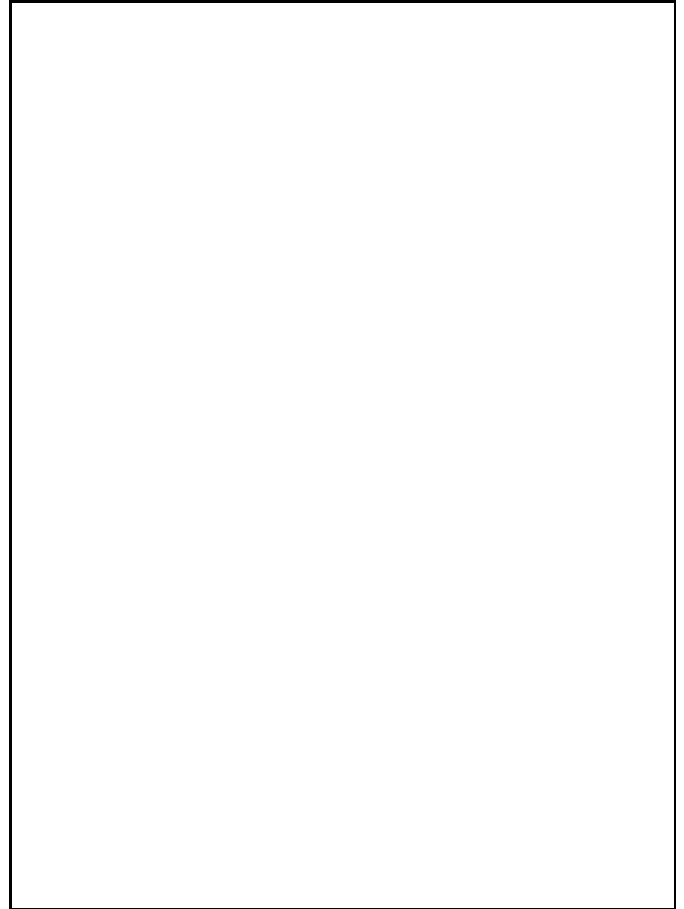


**Fig. 9.** The interstellar cooling function  $\mathcal{L}$  for various values of ionisation.

The cooling rate  $\Lambda$  is given by the product of the square of the number density and the interstellar cooling function  $\mathcal{L}$ :

$$\Lambda = n^2 \mathcal{L}$$

The cooling rate depends on the number density  $n$ , the temperature  $T$  and the degree of ionization. The ratio between the cooling time and heating time can be expressed in terms of the heating rate  $Q$  and the cooling rate  $\Lambda$ :

$$\frac{t_{cool}}{t_{heat}} = \left( \frac{nk_B T}{\Lambda} \right) / \left( \frac{nk_B T}{Q} \right) = \frac{Q}{\Lambda}$$

The heating rate  $Q = \eta j^2$  due to magnetic reconnection is taken from our simulations. Even if we use the maximum cooling rate of

$$\Lambda_{max} = n^2 \mathcal{L}_{max} = n^2 \cdot 10^{-21} \left[ \frac{\text{erg cm}^3}{\text{s}} \right]$$

which is only valid for temperatures of  $10^{4-5}$  K, the cooling is never efficient enough to restrict the magnetic heating in the whole temperature range we have in mind ( $T_i =$

$10^{2-6}$  K). This can be seen from Fig. 10, which shows the ratio  $\frac{Q}{\Lambda_{max}}$  of the heating rate  $Q$  to the maximum cooling rate  $\Lambda_{max}$  versus the initial temperature  $T_i$ : In the “low temperature-regime” with an initial temperature of a few hundred K this ratio is about  $10^3$ , i.e. the cooling time exceeds the corresponding heating time at least by a factor  $10^3$ . In a real plasma at low temperatures the degree of ionization is considerably smaller than unity, so the value of the cooling function for these temperatures is overestimated by several orders of magnitudes. Therefore the ratio between the cooling time and the heating time will be much larger than the value above. In the “high temperature case” with an initial temperature of  $9 \cdot 10^5$  K this ratio is even greater:  $\frac{Q}{\Lambda_{max}} \approx 10^{10}$  or  $t_{cool} \approx 10^{10} t_{heat}$ ! So, the cooling time is considerably greater than the corresponding heating time !

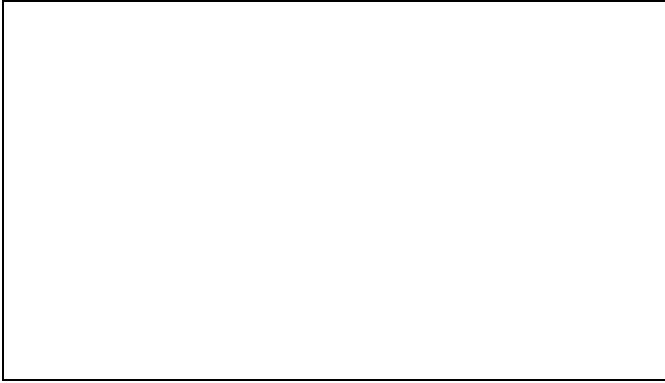


**Fig. 10.** The ratio between the heating rate  $Q$  and the maximum cooling rate  $\Lambda_{max}$  in dependence of the initial temperature  $T_i$ .

To construct a simple analytic expression of the heating rate, we use a plane sheet with length  $L$ , surface  $L^2$  and the thickness  $l$ .

The thickness  $l$  of a reconnection sheet has been determined by Parker (1979, p. 392): In the steady state Ohmic dissipation across the sheet is  $lj^2/\sigma$  is just sufficient to devour the influx of magnetic energy  $wB_0^2/8\pi$  from either side where  $w$  is the velocity with which two opposite fields move steadily towards each other. The total pressure  $p + \frac{B_0^2}{8\pi}$  is uniform across the sheet. The gas pressure  $p$  attains its highest value where  $B$  goes to zero. This pressure excess ejects plasma from the opposite fields, along the field lines. The velocity of expulsion is just equal to the Alfvén speed  $v_A$ . Conservation of fluid mass requires that the net magnetic field inflow balances the outflow

$$wL = v_A l. \tag{9}$$

where  $L$  denotes the width of the quasistationary current sheet. In terms of the magnetic Reynolds number  $R_M$

$$R_M = \frac{2L v_A}{\eta_R}, \tag{10}$$

( $\eta_R = c^2/(4\pi\sigma)$  denotes the resistive diffusion coefficient) and with

$$l \frac{j^2}{\sigma} = w \frac{B^2}{8\pi}, \tag{11}$$

one obtains

$$l = \frac{2L}{\sqrt{R_M}}, \tag{12}$$

and

$$w = \frac{2v_A}{\sqrt{R_M}}. \tag{13}$$

Inserting  $w$  and  $l$  into Eq. (11) and using  $Q = j^2/\sigma$  we end up with

$$Q = \frac{B^2 v_A}{8\pi L}. \tag{14}$$

By equating  $Q$  with the maximum value of the cooling function  $\mathcal{L}_{max}$ , we can determine what length scales can be heated up to the maximum value until cooling restricts the heating:

$$L \sim \frac{B^2}{8\pi} \frac{v_A}{10^{-21} n^2} \tag{15}$$

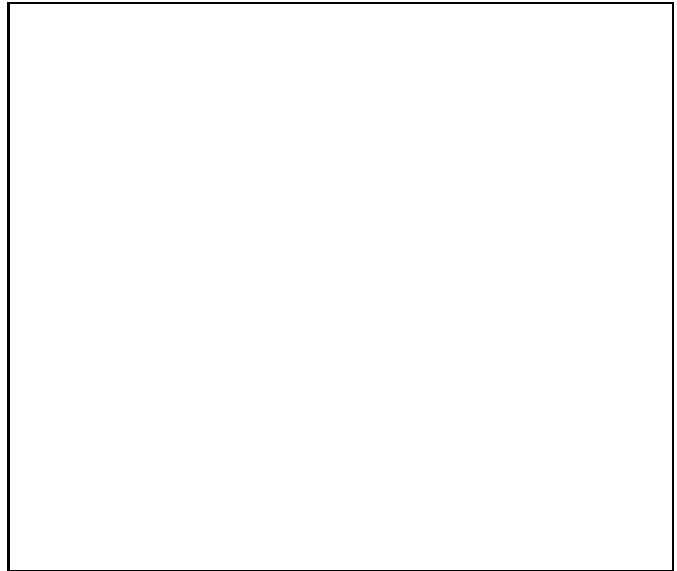


**Fig. 11.**  $L$  in dependence of the number density  $n$

Fig. 11 shows  $L$  for the density we have in mind. Obviously the heating is much more efficient than even the strongest cooling agent for the spatial scales we need to explain the X-ray temperatures connected with impacting HVCs  $\sim$  pc. Only very dense regions with densities of about  $10 \text{ cm}^{-3}$  can be influenced by cooling, but there we overestimate the cooling function by several orders of magnitudes, as can be seen from Fig. 9, since the high density regions are only partially ionized because of their small initial temperatures ( $\sim 100 \text{ K}$ ).

We know that magnetic reconnection is more effective in small localized regions, i.e. the thermal energy has to be transported by thermal conductive processes. During the interaction of a HVC with the galactic halo the gas will be heated up. Since the observations with ROSAT show that the X-ray emitting hot gas is restricted to an enclosed area, the typical time scale for thermal conductive processes has to be much larger than the heating time. The physics of heat transport in magnetized plasmas is still a matter of debate. Especially the influence of magnetic fields on the thermal conductivity  $\kappa$  is still unclear. The widespread belief that tangled magnetic fields reduce  $\kappa$  by several orders of magnitudes was shown to be highly questionable (Rosner & Tucker 1989). We therefore use the classical value of the thermal conductivity for a hydrogen plasma (Spitzer 1956):

$$\kappa \simeq 1.31 n_e \lambda_e k_B \left( \frac{k_B T_e}{m_e} \right)^{1/2}$$

with

$$\lambda_e = \frac{3^{3/2} (k_B T_e)^2}{4 \pi^{1/2} n_e e^4 \ln \Lambda}$$

$T_e$  is the electron temperature,  $n_e$  the number density and  $\ln \Lambda$  denotes the Coulomb logarithm, i.e. the ratio of largest to smallest impact parameters for the collisions. The conductivity time scale is approximately given by

$$t_{cond} \simeq \frac{n L_{\nabla T}^2 k_B}{\kappa}$$

where  $L_{\nabla T} := \frac{T}{|\nabla T|}$  is the length scale on which the temperature changes. So we find for the ratio between the conductivity time scale and the heating time:

$$\begin{aligned} \frac{t_{cond}}{t_{heat}} &\simeq \frac{4\pi^{1/2} e^4 \ln \Lambda m_e^{1/2}}{1.31 \cdot 3^{3/2} k_B^{7/2}} \frac{L_{\nabla T}^2 Q}{T_e^{7/2}} \\ &\simeq 2.1585 \cdot 10^6 \left[ \frac{\ln \Lambda}{40} \right] \frac{L_{\nabla T}^2 Q}{T_e^{7/2}} \end{aligned}$$

A ratio of about  $10^3$  between these time scales requires  $L_{\nabla T} \leq 5 \cdot 10^{-8} \text{ pc}$  for the low temperature gas and  $L_{\nabla T} \leq 5 \cdot 10^{-2} \text{ pc}$  for the high temperature regime! Since

the observed length scales are much larger,  $t_{cond}$  will exceed the heating time by a factor of more than  $10^3$ . Kerp & Güsten (1996, in prep.) detected a magnetic field located close to the X-ray brightest part of HVC 90.5+42.5-130 via HI 21cm Zeeman observations with the Effelsberg telescope with a linear size of about 10 pc. Such fields are well ordered and will substantially reduce the thermal conductivity perpendicular to the field lines. Thus, the hot gas in the boundary between HVC and halo is thermally well isolated from the halo.

## 5. Summary

We have investigated whether compressional heating of magnetized plasmas and magnetic reconnection can play important roles in the heating of cosmic plasmas. As an example we used the impact of a magnetized high-velocity cloud onto the magnetized galactic halo and the observed correlation with X-ray emission. The clouds move with velocities of about  $100 \text{ km s}^{-1}$  and heat a gas to higher temperatures than kinetically expectable (some  $10^5 \text{ K}$ !). Thus, we idealize the interaction of the cloud with the halo by a very general physical situation of two magnetized plasmas which encounter with a velocity corresponding to the observed HVC-speeds. Due to the high conductivity of both plasma components the first stage of the interaction is dominated by compression of the field lines perpendicular to the direction of motion of the cloud. This compression alone already increases the pressure and temperature of the material in the boundary layer between the cloud and halo. Due to internal motions inside the layer, the compressed field lines are stretched, twisted, strained and curled by plasma motions. Thereby magnetic field lines with antiparallel directions encounter. The subsequent chain of electrodynamic processes is known as magnetic reconnection and corresponds to a strongly enhanced dissipation of the kinetic energy stored in the compressed magnetic fields via Ohmic heating  $\propto j^2/\sigma$ . The interaction of two highly conducting plasmas provides both necessary conditions for enhanced Ohmic heating: first it leads to an increase of the current density  $j$  by compression and second if a critical current density is exceeded plasma instabilities are excited, which increase the collision frequency by many orders of magnitude, thereby reducing the electrical conductivity  $\sigma$  significantly.

We have shown that magnetic heating in low density plasmas is not restricted by even the most effective radiative cooling or heat conduction. The agitated plasma will always reach the maximal attainable temperature, deduced from the magnetic pressure  $B^2/8\pi$ . Our model explains the overall energetics and the observed temperatures.

Since both heating mechanisms - magnetic compression and magnetic reconnection - are unavoidable in magnetized plasmas which are agitated by randomly directed gas motions, we think that the dissipation of magnetic

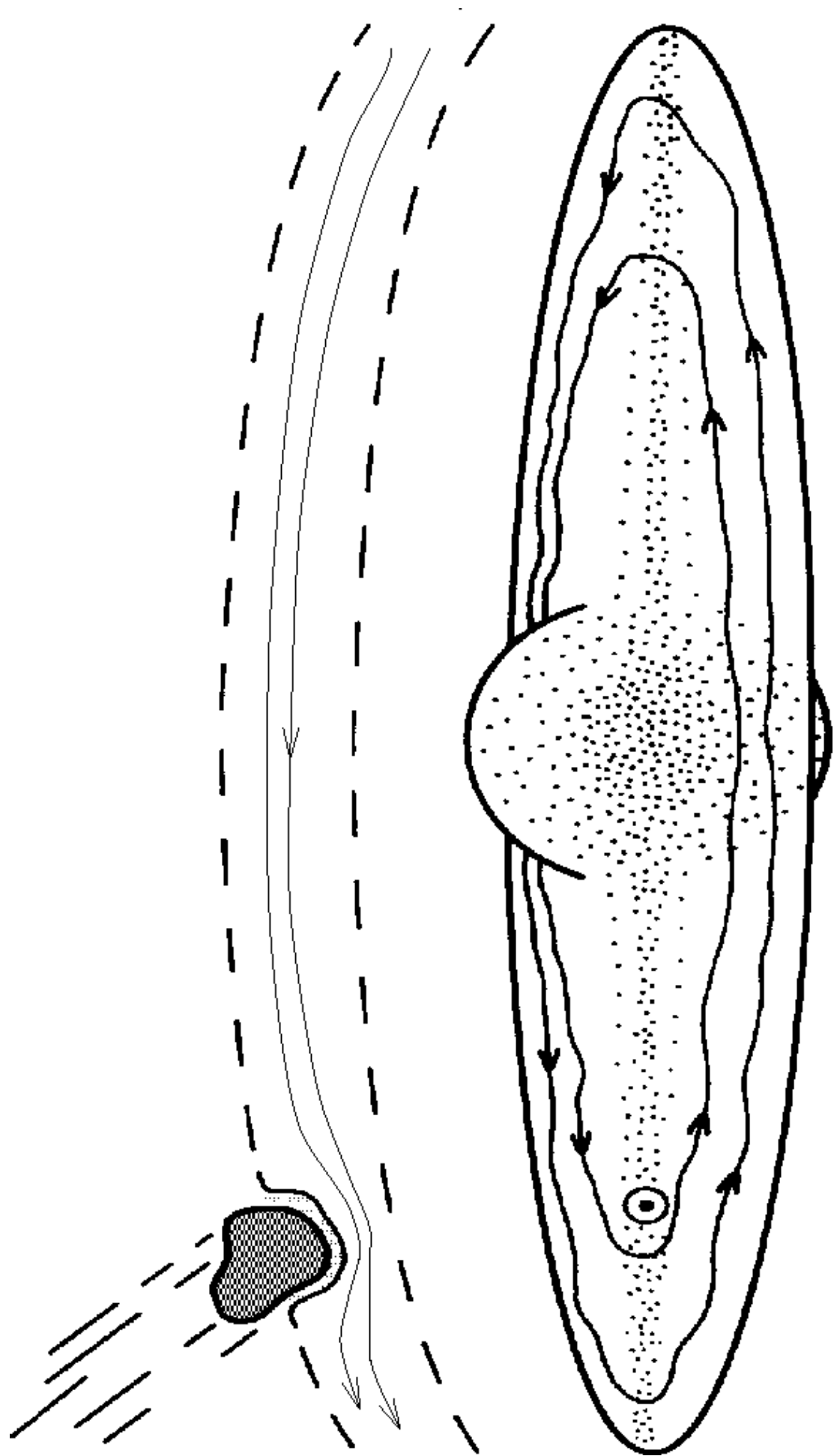
fields in cosmic plasmas presents a new possibility in the context of astrophysical heating and cooling processes. Since most of the astrophysical plasmas can be envisaged as highly conductive, any plasma motion is accompanied by the motion of magnetic field lines. Any velocity component perpendicular to the field lines compresses the magnetic field. This compression increases the magnetic pressure faster than the thermal pressure is enhanced, i.e.  $B \propto \rho$ ,  $B^2 \propto \rho^2$  and for isotropic compression  $B^2 \propto \rho^{4/3}$ . In any case the magnetic pressure becomes more and more important during the interaction of streaming plasmas. Since the magnetic pressure has its physical origin in the Lorentz-force density  $\propto \mathbf{j} \times \mathbf{B}$ , an enhancement of the magnetic pressure is synonymous with an increase of the current density and the dissipation rate. The actual location where this dissipation takes place depends on the field direction and the local electrical conductivity, which in turn depends on the current density! This electrodynamic coupling scenario allows the localized release of energy which has been stored in globally compressed magnetic field lines.

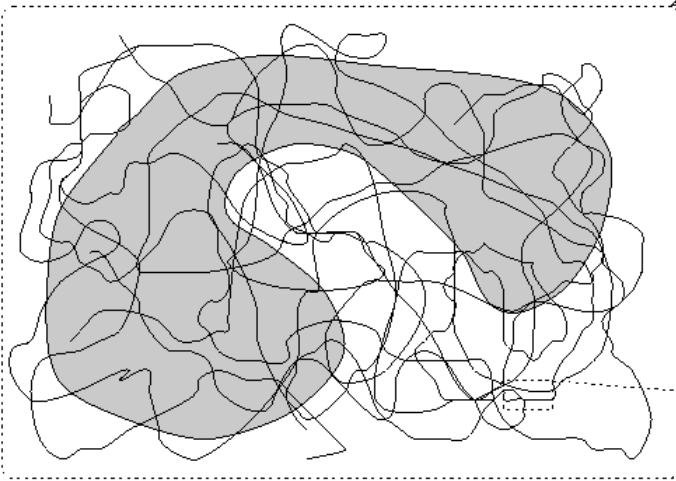
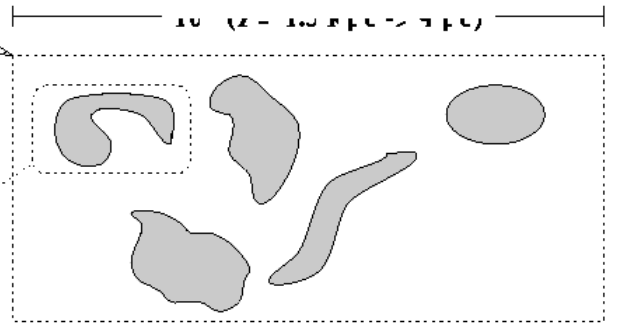
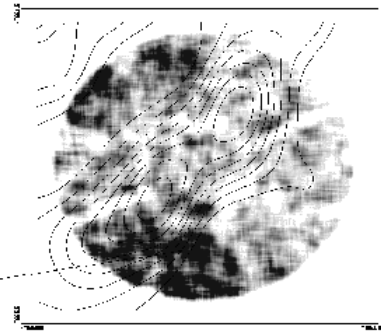
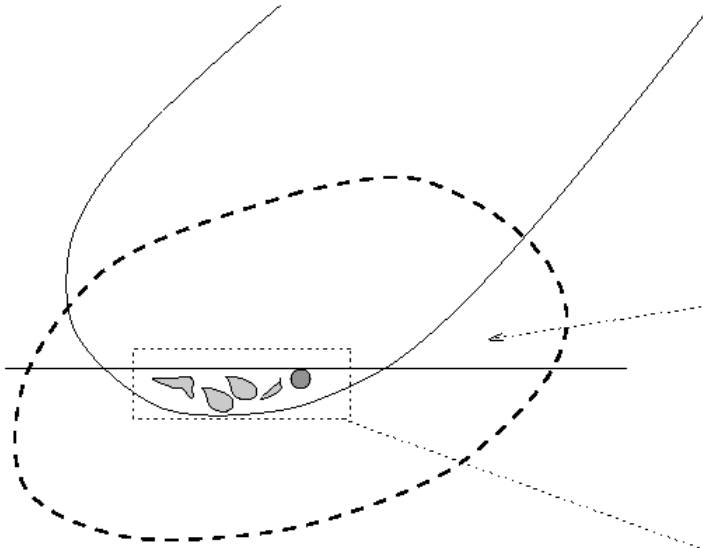
*Acknowledgements.* This work was supported by the Deutsche Forschungsgemeinschaft through the grant ME 745/18-1. F. Zimmer was supported by the Bennisgen-Foerder Award (1994) of the government of Nordrhein-Westfalen.

## References

- Beuermann, K., Kanbach, G., Berkhuijsen, E.M., 1985, A&A 153, 17  
 Biskamp, D., 1994, Phys. Rept. 237, 179  
 Dalgarno, A., McCray, R.A., 1972, ARA&A 10, 375  
 Dumke, M., Krause, M., Wielebinski, R., Klein, U., 1995, A&A 302, 691  
 Hartmann, D., Burton, W.B., 1995, An atlas of Galactic Neutral Hydrogen Emission, Cambridge University Press  
 Haslam, C.G.T., Salter, C.J., Stoffel, H., Wilson, W.E., 1982, A&AS 47, 1  
 Hirth, W., Mebold, U., Müller, P., 1985, A&A 153, 249  
 Kahn, F., 1981, in Dynamics of the Galactic Fountain, ed. F.D. Kahn, Reidel, p. 1  
 Kahn, F., 1991, IAU 144, 1  
 Kazès, I., Troland, T.H., Crutcher, R.M., 1991, A&A 245, L17  
 Kerp, J., Lesch, H., Mack, K.H., 1994, A&A 286, L13  
 Kerp, J., Mack, K.H., Egger, R., Pietz J., Zimmer F., Mebold U., Burton W.B., Hartmann D., 1996, A&A 312, 67  
 Kerp, J., Güsten, R., A&A (submitted)  
 Lesch, H., 1991, A&A 245, 48  
 Lesch H., Bender R., 1990, A&A 233, 417  
 Lesch, H., Dettmar, R., Mebold, U., Schlickeiser, R. (eds), 1996, Physics of Galactic Halos, Academic Press, Berlin  
 Mebold, U., Herbstmeier, U., Kalberla, P.M.W., Souvatzis, I., 1989, IAU Collq 120, eds. Tenorio-Tagle et al. p. 424  
 Mebold, U., Hirth, W., de Boer, K.S., 1991, in Proc. of "Hot Gas in the Galaxy", ed. Gondhelar, p. 64

- Muller, G.A., Oort, J.H., Raimond, E., 1963, Acad. Sci. Paris 257, 1661  
 Oort, J.H., 1970, A&A 7, 381  
 Otto, A., 1990, Comput. Phys. Commun., 59, 185  
 Parker, E.N., 1979, Cosmic Magnetic Fields, Oxford University Press  
 Pietz, J., Kerp, J., Kalberla, P.M.W., Mebold U., Burton W.B., Hartmann D., 1996, A&A 308, L37  
 Priest, E.R., 1985, Rep. Prog. Phys., 48, 955  
 Reynolds, R.J., 1991, IAU 144, 67  
 Rosner, R., Tucker, W.H., 1989, ApJ 338, 761  
 Sagdeev, R.Z., 1979, Rev. Mod. Phys. 51, 1  
 Schindler K., Hesse M., Birn J.: 1991, ApJ, 380, 293  
 Shapiro, V.D., Shevchenko, V.I., Cargill, P.J., Papadopoulos, K., 1994, JGR 99, 23735  
 Sotnikov, V.I., Shapiro, V.D., Shevchenko, V.I., 1978, Sov.Phys-JETP 51, 295  
 Spitzer, L., 1956, Physics of Fully Ionized Gases, Wiley, New York  
 Wakker, B.P., 1991, A&A 252, 433  
 Zimmer F., Birk G., Kerp J., Lesch H., 1996, Astrophysical Letters & Communications, Vol. 34, 193





10 μm

